Senescent cells and the dynamics of aging

Omer Karin[*1], Amit Agrawal[*1], Ziv Porat[2], Valery Krizhanovsky[#1], Uri Alon[#1]

[1]Dept. Molecular Cell Biology, Weizmann Institute of Science, Rehovot, Israel, 76100

[2]Dept. of Biological Services, Weizmann Institute of Science, Rehovot, Israel, 76100

[*]equal contribution

[#]corresponding authors (uri.alon@weizmann.ac.il, valery.krizhanovsky@weizmann.ac.il)

Abstract

Aging is studied at two levels that are rarely linked: the level of cellular processes and the demographic level. It is unclear how cellular mechanisms can quantitatively explain nearly universal demographic laws, such as the Gompertz law in which risk of death rises exponentially with age. Here we unify these levels using mathematical modeling and experiments in mice, showing how the Gompertz law emerges quantitatively from the stochastic dynamics of senescent cells (SnC), damaged cells that accumulate with age and are causal for aging. We show that SnC have rapid turnover with a half-life of days in young mice. However, they slow their own removal to a half-life of weeks in old mice. This leads to critical-slowing-down that generates persistent fluctuations that can quantitatively explain the Gompertz law. This opens the way to integrate the cellular and demographic levels of aging, and to understand interventions that affect the healthy lifespan.

Introduction

As organisms age, intracellular damage accumulates (Enge et al., 2017; Hoeijmakers, 2009), leading to cellular senescence and the decline of physiological function. In many species, including mice and humans, risk of death rises exponentially with age over several orders of magnitude, a relation known as the Gompertz law (Gompertz, 1825; Kirkwood, 2015), showing a slowdown at very old ages. Even genetically identical organisms raised in the same conditions die at different times according to the Gompertz law, suggesting a non-genetic stochastic component to mortality (Stroustrup et al., 2016). However, the cellular identity of this stochastic component is unclear. Thus, although much is known about cellular mechanisms of aging, the Gompertz law has no explanation at the cellular level (Figure 1A).

To address this, we combine experiments and mathematical modelling. We build on recent findings that a major driver of mammalian aging is the accumulation of senescent cells (SnC) (Baker et al., 2016; Campisi and d'Adda di Fagagna, 2007; López-Otín et al., 2013; Muñoz-Espín and Serrano, 2014; Ogrodnik et al., 2018; Salama et al., 2014). SnC are damaged cells that stop dividing and secrete pro-inflammatory signals (He and Sharpless, 2017; Von Zglinicki et al., 2005) (Figure 1B). They are identified using markers such as p16 (Burd et al., 2013; Demaria et al., 2014; Liu et al., 2009) and SA-β-Gal (Biran et al., 2017; Debacq-Chainiaux et al., 2009; Dimri et al., 1995). SnC are produced in many tissues as a result of cellular stress, including DNA damage, damaged telomeres, and oxidative stress (Biran et al., 2017; Childs et al., 2015, 2016; Demaria et al., 2015; Franceschi and Campisi, 2014; Freund et al., 2010; Muñoz-Espín and Serrano, 2014; Van Deursen, 2014; Young and Narita, 2009). The number of SnC increases exponentially with age in mice and humans in many tissues (Biran et al., 2017; Burd et al., 2013; Herbig et al., 2006; Liu et al., 2009; Melk et al., 2004; Sofue et al., 2018; Zhou et al., 2008).

Accumulation of SnC is causal for aging in mice: continuous targeted elimination of whole-body SnC increases mean lifespan by 25%, attenuates age-related deterioration of heart, kidney, and fat, delays cancer development (Baker et al., 2016). SnC removal causes improvement in diverse age-related conditions, including vascular disease (Childs et al., 2016; Roos et al., 2016), neurodegeneration (Bussian et al., 2018), osteoarthritis (Jeon et al., 2017), fatty liver disease (Ogrodnik et al., 2017), sarcopenia (Baker et al., 2016; Chang et al., 2016), cachexia (Xu et al., 2015), idiopathic pulmonary fibrosis (Schafer et al., 2017), and chronic lung inflammation (Sagiv et al., 2018). SnC exert these negative effects by impairing tissue function and regeneration, modifying the extracellular matrix, and causing chronic inflammation (Childs et al., 2016; Demaria

et al., 2015; Franceschi and Campisi, 2014; Freund et al., 2010; He and Sharpless, 2017; Muñoz-Espín and Serrano, 2014; Van Deursen, 2014; Young and Narita, 2009).

These studies indicate that total SnC abundance is a critical variable underlying the aging process. We therefore asked whether the dynamics of SnC can explain the Gompertz law of mortality and other population-level features. To address this question, we needed to determine the dynamics of SnC production and removal, which are currently unknown (He and Sharpless, 2017; López-Otín et al., 2013).

Results

Scan of circuits for SnC accumulation dynamics

To understand the dynamics of SnC, we scanned a wide class of models of SnC dynamics, and, as described below, compared these models to longitudinal SnC trajectories (Burd et al., 2013) and to direct SnC induction experiments in mice (Figure 1C).

The models describe production and removal of SnC. They differ from each other in the way that production and removal rates are affected by age and by SnC abundance (Figure 1C). The models describe all combinations of four possible mechanisms for SnC accumulation (i) SnC production rate can increase with age due accumulation of mutations (Enge et al., 2017; Hoeijmakers, 2009), telomere damage and other forms of intracellular damage that trigger cellular senescence (d'Adda di Fagagna, 2008; di Fagagna et al., 2003; Karlseder et al., 2002; Shay and Wright, 2004) (ii) SnC can catalyze their own production by paracrine and bystander effects (Acosta et al., 2013; Nelson et al., 2012, 2018), (iii) SnC removal rate can decrease with age due to age-related decline in immune surveillance functions (Aw et al., 2007; Collerton et al., 2012; Solana et al., 2012), and (iv) high SnC levels can saturate their own immune surveillance mechanisms. This leads to a class of 16 different circuits (Figure 1C) with all combinations of these dependencies, in addition to basal parameters for production and removal. Each of these models has rate constants, which are currently uncharacterized.

A minimal circuit captures longitudinal SnC dynamics in mice

To find which of the model mechanisms best describes SnC dynamics, we compared them to longitudinal data on SnC abundance in mice collected by Burd et al. (Burd et al., 2013). SnC abundance was measured using a luciferase reporter for the expression of $p16^{INK4a}$, a biomarker for senescent cells (Baker et al., 2011; Liu et al., 2009). Total body luminescence (TBL) was monitored

every 8 weeks for 33 mice, from early age (8 weeks) to middle-late adulthood (80 weeks) (Figure 2A).

We tested how well each model describes the longitudinal SnC trajectories by finding the maximum likelihood parameters for each of the 16 models, adjusting for number of parameters (Supplementary Section 1 and Section 2). A principle emerges from this comparison: in order to capture the longitudinal dynamics, the mechanism must include saturation of removal rate, and have rapid turnover of SnC on the timescale of a few days in young mice. The simplest model that describes the data has only two interactions (Figure 2B): SnC production rate increases linearly with age, and SnC slow down their own removal rate by saturating the removal process, similar to saturation of an enzyme by its substrate. We call this the saturating removal model (SR model).

The SR model captures the accelerating rise of mean SnC abundance with age in the longitudinal data (Figure 2C), the increasing SnC variability between individuals (Figure 2D), and the SnC distributions between equal-aged individuals (Figure 2E) which are skewed to the right (Fig 2F).

Importantly, the SR model also captures the fact that SnC fluctuations become more persistent with age, as evidenced by an increasing correlation between subsequent measurements (Figure 2G, $p<0.01$): individuals with higher (or lower) than average SnC levels stay higher (or lower) for longer periods with age. Models without saturation of removal show a poor overall fit (light-red line in Figure 2C).

The maximum likelihood parameters of the SR model provide quantitative predictions for SnC half-lives: (i) SnC turnover is rapid in young mice (3 month-old) with a half-life of about 5±1 day. (ii) Turnover rate slows down with age, so that SnC half-life is about 25±6 days at 22 months.

Measurement of senescent cell turnover in young and old mice

We experimentally tested these predictions in mice, by inducing the formation of senescent cells and measuring their half-life. To induce senescence in mice lungs we used intratracheal bleomycin administration (Figure 3A). Bleomycin is a DNA-damaging agent that induces cellular senescence in the lung epithelium (Aoshiba et al., 2003; Biran et al., 2017) a few days after drug treatment.

We quantified the fraction of senescent lung epithelial cells at different time points following bleomycin administration (Figure 3A) using imaging flow cytometry. Epithelial SnC

were defined as positive for a senescent cell marker (SA-β-Gal) and an epithelial marker (pan-Cytokeratin pCK). This cell population was also HMGB1 nuclear negative, as expected in senescent cells (Biran et al., 2017; Davalos et al., 2013), and was previously shown (Biran et al., 2017) to be non-proliferative (negative Ki67 assay) (see Supplementary Section 3, Figure S1).

We first tested the prediction that turnover is rapid in young mice (Figure 3B). In 3 month-old mice, SnC decayed with a half-life of $\tau = 4.7$ days ($\tau^{-1} = 0.21 \pm 0.07\ days^{-1}$) and reached their baseline level within less than a month (Figure 3C). This result indicates that, as predicted, SnC levels in young mice are in a relatively fast dynamic balance of production and removal.

To test the prediction that removal slows with age (Figure 3B), we performed the bleomycin treatment in old mice (22 month-old). In these mice, the baseline level of SnC was about 5-fold higher than in young mice (Figure 3D). In the old mice, SnC decayed with a half-life of $\tau =$ 18 days ($\tau^{-1} = 0.055 \pm 0.035\ days^{-1}$), which was slower than that of young mice, as predicted (Figure 3B).

These turnover measurements quantitatively agreed with the predictions of the SR model (Figure 3D, Supplementary Section 4 and Figure S2) with no additional fit. Notably, this agreement occurred despite the use of distinct SnC markers in the two data sets (SA-β-Gal in the bleomycin experiment vs. $p16^{INK4A}$-luciferase in the longitudinal experiment), indicating consistency between the measurement methods.

The SR model shows persistent fluctuations with age due to critical slowing down

These results suggest a core mechanism in which SnC accumulate because their production rate rises with age, and SnC saturate their own removal (Figure 4A). To understand how this mechanism works, consider the rate plot in Figure 4B, showing SnC production and removal curves as a function of SnC abundance. The crossing point of the curves is where production equals removal, and is hence the SnC steady-state level. At young ages, production rate is low, resulting in a low steady-state SnC level (Figure 4A). Production rate rises with age, and SnC concentrations increasingly saturate the removal capacity (Figure 4AB), causing the SnC steady-state to shift to ever higher levels. This results in an accelerating rise of SnC abundance with age.

Figure 4B also helps visualize the speed at which SnC return to steady-state after a perturbation. This speed is the distance between the curves near the crossing point, production minus removal (double-arrowed lines, Figure 4A). Young mice have a large distance between the curves, and hence rapid return to steady-state. Their removal mechanisms thus have spare capacity.

Old mice have a short distance between the curves, due to the saturation of removal, and hence a slower return to steady state. Importantly, the slower return causes stochastic fluctuations to last longer before returning to steady-state, a phenomenon known as critical slowing down (Scheffer et al., 2009). This slowdown causes larger and more persistent variation between individuals with age (Figure 2G).

The Gompertz law of mortality emerges from SnC dynamics

Equipped with an understanding of SnC dynamics, we next asked whether SnC dynamics can explain the empirical distribution of mortality times described by the Gompertz law (Kirkwood, 2015). To connect SnC dynamics and mortality, we need the relationship between SnC abundance and risk of death (Burd et al., 2013). The precise relationship is currently unknown. Since removing SnC from mice increases mean lifespan (Baker et al., 2016) and ameliorates aging-related decline including the major pathologies that cause mortality, and adding SnC to mice increases risk of death (Xu et al., 2018), we reasoned that risk of death p should increase with SnC abundance, $p(X)$. For example, death can be modeled to occur when SnC exceed a threshold level X_C (Weitz and Fraser, 2001), representing a collapse of an organ system or a tipping point such as sepsis. We use this assumption to demonstrate our approach, because it provides analytically solvable results. Other functions $p(X)$ provide similar conclusions (see Supplementary Section 2 and Figure S3).

The SR model analytically provides the Gompertz law, including the observed deceleration of mortality rates at old ages (Figure 5, Supplementary Section 2). The model gives a good fit to the mouse mortality curve (Figure 5AB, see Supplementary Section 1 for details). Notably, it does so with parameters that agree with the present experimental half-life measurements and longitudinal SnC data (Supplementary Information 1).

A good description of human mortality data, including the deceleration at old ages, is provided by the same parameters as in mice, except for a 60-fold slower increase in SnC production rate with age (Figure 5C, Supplementary Section 5). This slower increase in SnC production rate can be due to improved DNA maintenance in humans compared to mice (MacRae et al., 2015). We conclude that the SR mechanism for SnC dynamics provides a cellular mechanism for population-level mortality (Figure 5D), based on the persistent noise in SnC levels caused by the saturation of removal rates.

Discussion

We present a parametrized model for the dynamics of senescent cell accumulation throughout the lifespan that can explain the Gompertz law, where risk of death increases exponentially with age. The model was derived from a scan of a wide class of mechanisms to capture longitudinal SnC measurements in mice. We tested the model predictions that SnC rapidly turn over with a half-life of about 5 days in young mice, but SnC removal slows down dramatically in old mice, by in-vivo perturbation experiments of SnC in mice, finding excellent agreement.

The model is based on a linear increase in SnC production and a saturation of removal rate at high SnC levels. The saturation creates a critical-slowing-down effect, in which fluctuations in SnC last longer with age, generating widening individual differences in SnC accumulation. The generality of the model suggests that it may also be applicable to study aging dynamics in organisms without senescent cells, such as *C. elegans*, that also show the Gompertz law (Stroustrup et al., 2016; Vaupel, 1998). The approach can be extended by considering X as cellular damage that saturates its own removal, such as protein damage (Labbadia and Morimoto, 2015) that saturates proteostatic mechanisms.

The present results bear on the use of drugs that eliminate SnC, known as senolytics (Baar et al., 2017; Fuhrmann-Stroissnigg et al., 2017; Hwang et al., 2018; Kirkland and Tchkonia, 2015; Kirkland et al., 2017; Ovadya and Krizhanovsky, 2018; Scudellari, 2017; Xu et al., 2018; Yosef et al., 2016; Zhu et al., 2015, 2016, 2017). To reduce toxicity concerns, it is important to establish regimes of low dose and large inter-dose spacing (Kirkland and Tchkonia, 2015; Ovadya and Krizhanovsky, 2018; Yosef et al., 2016). The model provides a rational basis for scheduling senolytic drug administrations. Specifically, treatment should start at old age, and can be as infrequent as the SnC turnover time (~month in old mice) and still be effective (Supplementary Section 6).

In summary, we propose a quantitative link between cellular mechanisms and population-level mortality laws based on SnC dynamics. SnC show persistent stochastic variability caused by critical slowing down that provides a possible basis for the non-genetic variation in mortality observed in genetically identical organisms and in humans (Biran et al., 2017; Helman et al., 2016; Liu et al., 2009). Furthermore, because SnC reduce their own removal rate, drugs that remove senescent cells can have a double benefit: an immediate benefit from a reduced SnC load, and a longer-term benefit from increased SnC removal rate. Similarly, interventions that increase removal capacity (for example, by augmenting immune surveillance of SnC (Ovadya and Krizhanovsky, 2018)) are predicted to be an effective approach to reduce SnC levels and increase health-span.

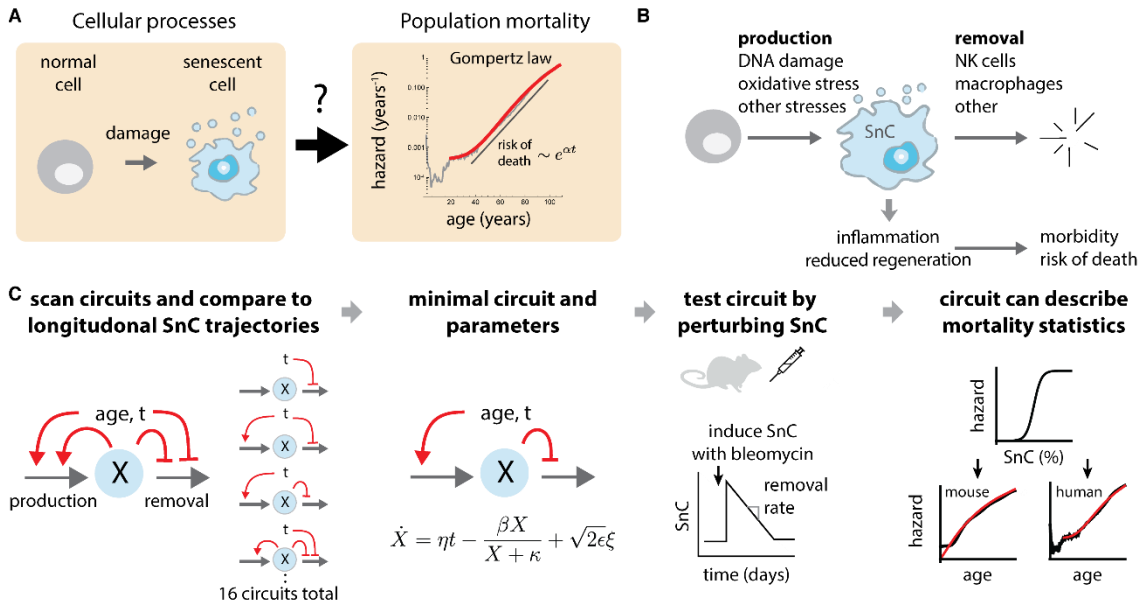

Figure 1. Approach for linking the cellular and population levels of aging. (A) The link between cellular damage mechanisms and population-level mortality statistics is unclear. (B) Many forms of cellular damage lead to SnC production. SnC are cleared by immune mechanisms, and secrete factors that lead to morbidity. (C) We scan a wide class of models for SnC dynamics, and compare them to longitudinal SnC data and direct SnC perturbation experiments to establish a minimal model for SnC stochastic dynamics and its rate constants. We then show that this model and rate constants can explain the Gompertz law.

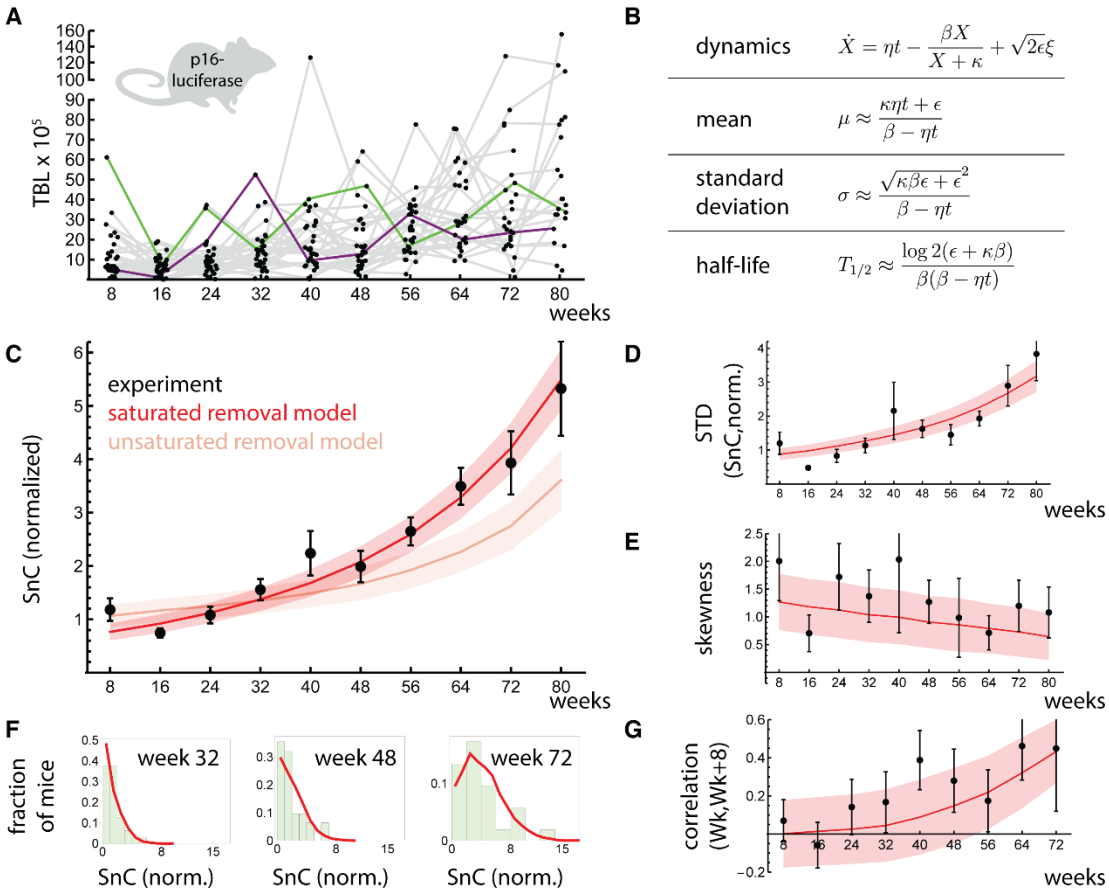

Figure 2. Saturated-removal (SR) model captures longitudinal SnC trajectories in mice. (A) Luminescence of p16-luciferase in mice. Grey lines connect data from the same individual mice. (B) SR model equations and their approximate analytical solutions. The SR model captures (C) the mean SnC abundance, (D) standard deviation of SnC abundance, (E) skewness and shape (F) of the distributions between equal-aged individuals, (G) correlation between subsequent measurements on the same individuals. TBL was normalized to give a mean abundance of $1[AU]$ at young ages. Maximum likelihood parameters are: $\eta = 0.15[AU]\, day^{-1} year^{-1}$, $\beta = 0.27\, day^{-1}$, $\kappa = 1.1[AU]$, $\epsilon = 0.14\, [AU]^2 day^{-1}$. Orange line: unsaturated removal (USR) model with best-fit parameters ($\frac{dX}{dt} = \eta_0 - (\beta_0 - \beta_1 t)X + \sqrt{2\epsilon}\xi$, $\eta_0 = 0$, $\beta_0 = 0.07\, day^{-1}$, $\beta_1 = 0.044\, day^{-1} year^{-1}$, $\epsilon = 0.22\, [AU]^2 day^{-1}$). Mean and standard error (light red, orange regions) are from bootstrapping.

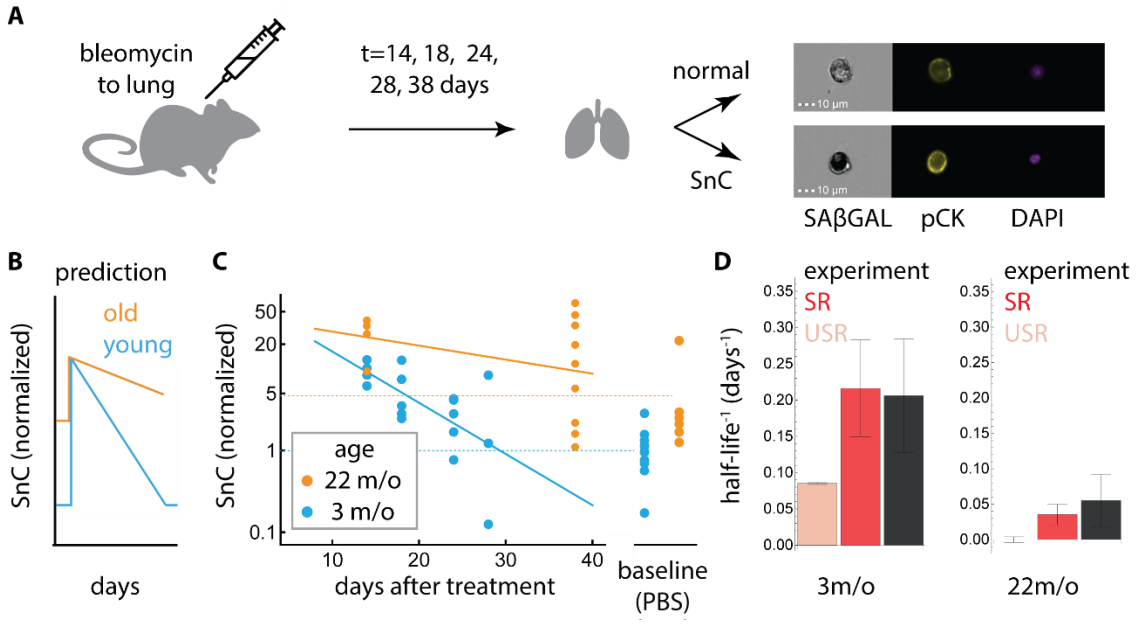

Figure 3. SnC half-life measurements in mice support SR model predictions. (A) Bleomycin or PBS was introduced by intratracheal installation to mice on day 0. Lungs were analyzed on the indicated days thereafter. Representative images of lung cells analyzed by imaging flow cytometry show how senescent epithelial cells were identified, using SA-β-Gal, Pan-Cytokeratin (pCK), and DAPI staining. SnC removal rate was estimated by fitting a log-linear model. (B) The SR model predicts that SnC rapidly return to baseline in young mice and that removal is slower in old mice. (C) Fraction of SnC in mice lung after treatment with bleomycin (1.5U/Kg). In young mice, SnC levels return to baseline with a half-life of about 5 days. In old mice, baseline SnC levels are about 5-fold higher, and SnC removal rate is slower than in young mice (p=0.038). (D) SnC removal rates (half-life^{-1}) for young and old mice (mean and SE, black) agree with the SR model predictions (red, mean and SE were calculated by bootstrapping, see Methods). The best-fit model without saturated removal (USR) shows a poor prediction (orange).

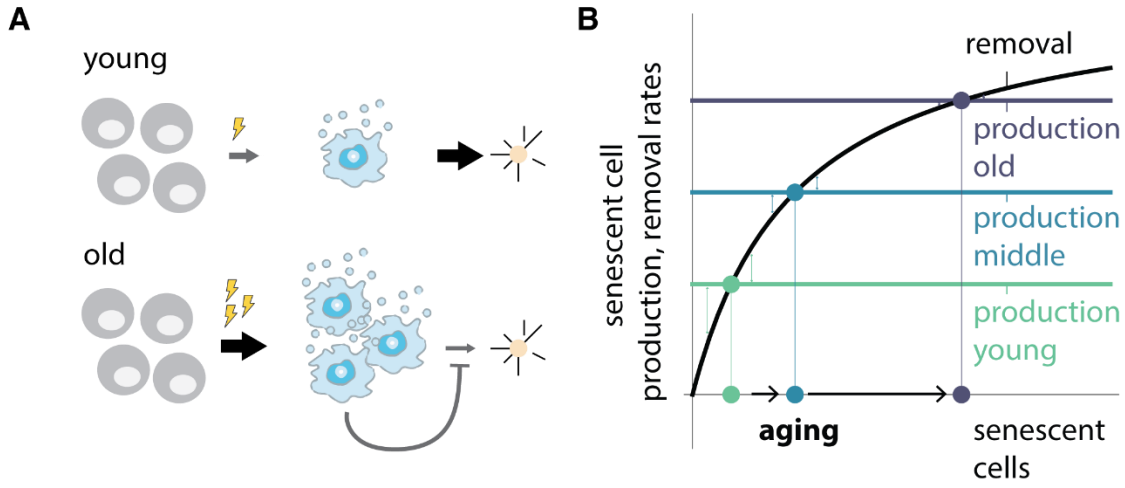

Figure 4. Saturating removal and increasing production lead to accelerated SnC abundance with age and persistent SnC fluctuations. (A) With age, production rate increases, SnC levels rise and increasingly saturate their own removal mechanism, further amplifying their rate of increase. (B) Rate plot of removal and production as a function of SnC abundance. Steady-state occurs when production and removal curves cross (dots). As production rises, SnC levels accelerate to higher abundance. At old ages, the spare capacity for removal- the distance between production and removal curves- shrinks, so that SnC perturbations last longer, leading to persistent fluctuations. These fluctuations cause non-genetic variation between individuals that lasts for long times.

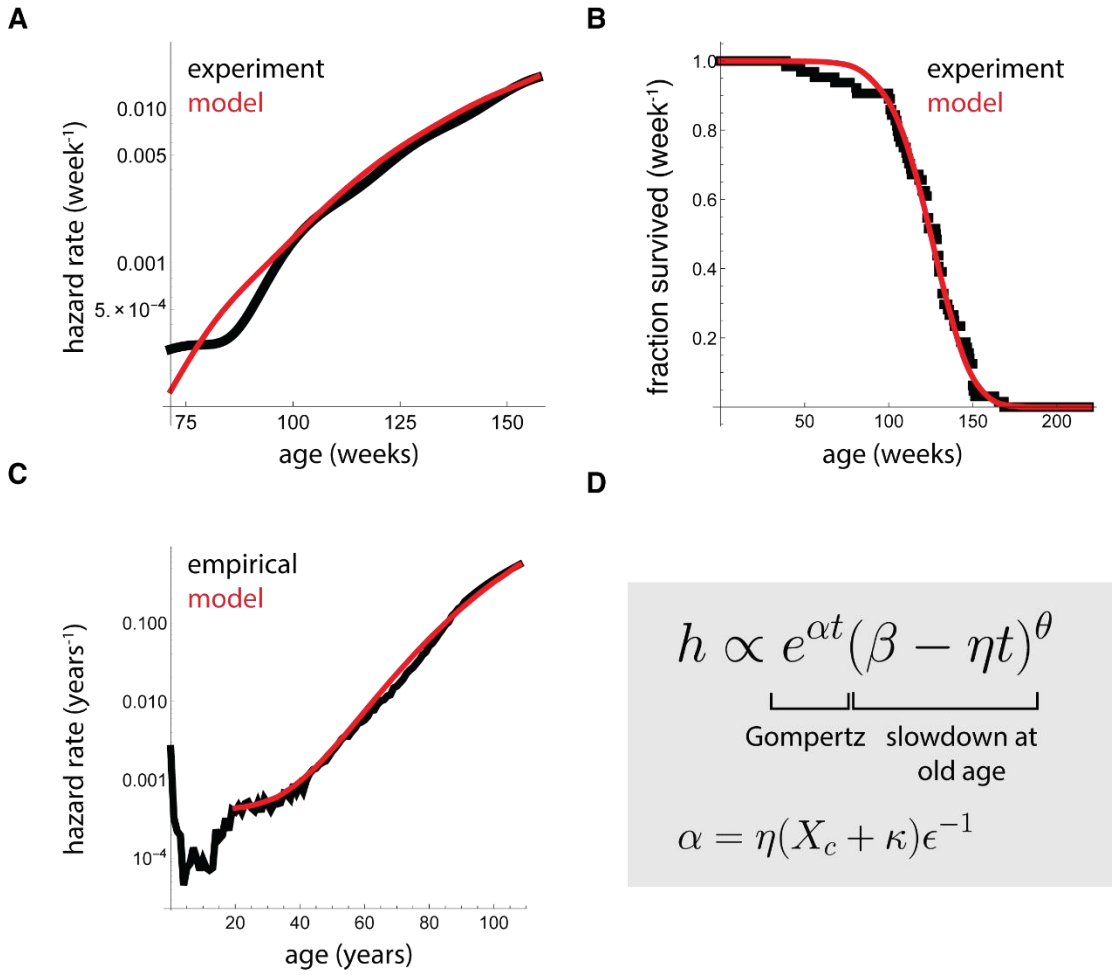

Figure 5. SnC dynamics can explain the Gompertz law of mortality. The SR model analytically provides the Gompertz law, assuming that death occurs when SnC exceed a threshold X_c. (A, B) mouse mortality (black, C57BL/6J mice obtained from the Mouse Phenome Database (Grubb et al., 2014)) is well fit by the SR model (red) with parameters consistent with the data of Figures 1, 2 (see Supplementary Information 1 for parameters). (C) The model with added age-independent extrinsic mortality ($0.4 \cdot 10^{-3} year^{-1}$) (red) matches human mortality statistics (Barbieri et al., 2015) (black). (D) Approximate analytical solution for mortality in the SR model shows the Gompertz law and deceleration at old ages.

Acknowledgments

U.A. is the incumbent of the Abisch-Frenkel chair. O.K. is an Azrieli Fellow. This work was supported by grants to V.K. from the European Research Council under the European Union's FP7 and H2020 Programs and the Israel Science Foundation.

References

Acosta, J.C., Banito, A., Wuestefeld, T., Georgilis, A., Janich, P., Morton, J.P., Athineos, D., Kang, T.-W., Lasitschka, F., Andrulis, M., et al. (2013). A complex secretory program orchestrated by the inflammasome controls paracrine senescence. Nat. Cell Biol. *15*, 978–990.

Aoshiba, K., Tsuji, T., and Nagai, A. (2003). Bleomycin induces cellular senescence in alveolar epithelial cells. Eur. Respir. J. *22*, 436–443.

Aw, D., Silva, A.B., and Palmer, D.B. (2007). Immunosenescence: emerging challenges for an ageing population. Immunology *120*, 435–446.

Baar, M.P., Brandt, R.M.C., Putavet, D.A., Klein, J.D.D., Derks, K.W.J., Bourgeois, B.R.M., Stryeck, S., Rijksen, Y., van Willigenburg, H., Feijtel, D.A., et al. (2017). Targeted Apoptosis of Senescent Cells Restores Tissue Homeostasis in Response to Chemotoxicity and Aging. Cell *169*, 132-147.e16.

Baker, D.J., Wijshake, T., Tchkonia, T., LeBrasseur, N.K., Childs, B.G., van de Sluis, B., Kirkland, J.L., and van Deursen, J.M. (2011). Clearance of p16Ink4a-positive senescent cells delays ageing-associated disorders. Nature *479*, 232–236.

Baker, D.J., Childs, B.G., Durik, M., Wijers, M.E., Sieben, C.J., Zhong, J., Saltness, R.A., Jeganathan, K.B., Verzosa, G.C., Pezeshki, A., et al. (2016). Naturally occurring p16(Ink4a)-positive cells shorten healthy lifespan. Nature *530*, 184–189.

Barbieri, M., Wilmoth, J.R., Shkolnikov, V.M., Glei, D., Jasilionis, D., Jdanov, D., Boe, C., Riffe, T., Grigoriev, P., and Winant, C. (2015). Data Resource Profile: The Human Mortality Database (HMD). Int. J. Epidemiol. *44*, 1549–1556.

Biran, A., Zada, L., Abou Karam, P., Vadai, E., Roitman, L., Ovadya, Y., Porat, Z., and Krizhanovsky, V. (2017). Quantitative identification of senescent cells in aging and disease. Aging Cell *16*, 661–671.

Burd, C.E., Sorrentino, J.A., Clark, K.S., Darr, D.B., Krishnamurthy, J., Deal, A.M., Bardeesy, N., Castrillon, D.H., Beach, D.H., and Sharpless, N.E. (2013). Monitoring Tumorigenesis and Senescence In Vivo with a p16INK4a-Luciferase Model. Cell *152*, 340–351.

Bussian, T.J., Aziz, A., Meyer, C.F., Swenson, B.L., van Deursen, J.M., and Baker, D.J. (2018). Clearance of senescent glial cells prevents tau-dependent pathology and cognitive decline. Nature *562*, 578–582.

Campisi, J., and d'Adda di Fagagna, F. (2007). Cellular senescence: when bad things happen to good cells. Nat. Rev. Mol. Cell Biol. *8*, 729–740.

Chang, J., Wang, Y., Shao, L., Laberge, R.-M., Demaria, M., Campisi, J., Janakiraman, K., Sharpless, N.E., Ding, S., Feng, W., et al. (2016). Clearance of senescent cells by ABT263 rejuvenates aged hematopoietic stem cells in mice. Nat. Med. *22*, 78–83.

304 Childs, B.G., Durik, M., Baker, D.J., and Van Deursen, J.M. (2015). Cellular senescence in aging
305 and age-related disease: from mechanisms to therapy. Nat. Med. *21*, 1424.

306 Childs, B.G., Baker, D.J., Wijshake, T., Conover, C.A., Campisi, J., and van Deursen, J.M. (2016).
307 Senescent intimal foam cells are deleterious at all stages of atherosclerosis. Science *354*, 472–
308 477.

309 Collerton, J., Martin-Ruiz, C., Davies, K., Hilkens, C.M., Isaacs, J., Kolenda, C., Parker, C., Dunn,
310 M., Catt, M., and Jagger, C. (2012). Frailty and the role of inflammation, immunosenescence and
311 cellular ageing in the very old: cross-sectional findings from the Newcastle 85+ Study. Mech.
312 Ageing Dev. *133*, 456–466.

313 Davalos, A.R., Kawahara, M., Malhotra, G.K., Schaum, N., Huang, J., Ved, U., Beausejour, C.M.,
314 Coppe, J.-P., Rodier, F., and Campisi, J. (2013). p53-dependent release of Alarmin HMGB1 is a
315 central mediator of senescent phenotypes. J. Cell Biol. *201*, 613–629.

316 Debacq-Chainiaux, F., Erusalimsky, J.D., Campisi, J., and Toussaint, O. (2009). Protocols to detect
317 senescence-associated beta-galactosidase (SA-βgal) activity, a biomarker of senescent cells in
318 culture and in vivo. Nat. Protoc. *4*, 1798.

319 Demaria, M., Ohtani, N., Youssef, S.A., Rodier, F., Toussaint, W., Mitchell, J.R., Laberge, R.-M.,
320 Vijg, J., Van Steeg, H., and Dollé, M.E. (2014). An essential role for senescent cells in optimal
321 wound healing through secretion of PDGF-AA. Dev. Cell *31*, 722–733.

322 Demaria, M., Desprez, P.Y., Campisi, J., and Velarde, M.C. (2015). Cell autonomous and non-
323 autonomous effects of senescent cells in the skin. J. Invest. Dermatol. *135*, 1722–1726.

324 Dimri, G.P., Lee, X., Basile, G., Acosta, M., Scott, G., Roskelley, C., Medrano, E.E., Linskens, M.,
325 Rubelj, I., and Pereira-Smith, O. (1995). A biomarker that identifies senescent human cells in
326 culture and in aging skin in vivo. Proc. Natl. Acad. Sci. *92*, 9363–9367.

327 Enge, M., Arda, H.E., Mignardi, M., Beausang, J., Bottino, R., Kim, S.K., and Quake, S.R. (2017).
328 Single-Cell Analysis of Human Pancreas Reveals Transcriptional Signatures of Aging and Somatic
329 Mutation Patterns. Cell *171*, 321-330.e14.

330 d'Adda di Fagagna, F. (2008). Living on a break: cellular senescence as a DNA-damage response.
331 Nat. Rev. Cancer *8*, 512–522.

332 di Fagagna, F. d'Adda, Reaper, P.M., Clay-Farrace, L., Fiegler, H., Carr, P., von Zglinicki, T.,
333 Saretzki, G., Carter, N.P., and Jackson, S.P. (2003). A DNA damage checkpoint response in
334 telomere-initiated senescence. Nature *426*, 194.

335 Franceschi, C., and Campisi, J. (2014). Chronic inflammation (inflammaging) and its potential
336 contribution to age-associated diseases. J. Gerontol. A. Biol. Sci. Med. Sci. *69 Suppl 1*, S4-9.

337 Freund, A., Orjalo, A.V., Desprez, P.-Y., and Campisi, J. (2010). Inflammatory networks during
338 cellular senescence: causes and consequences. Trends Mol. Med. *16*, 238–246.

339 Fuhrmann-Stroissnigg, H., Ling, Y.Y., Zhao, J., McGowan, S.J., Zhu, Y., Brooks, R.W., Grassi, D.,
340 Gregg, S.Q., Stripay, J.L., Dorronsoro, A., et al. (2017). Identification of HSP90 inhibitors as a
341 novel class of senolytics. Nat. Commun. *8*.

342 Gompertz, B. (1825). On the Nature of the Function Expressive of the Law of Human Mortality,
343 and on a New Mode of Determining the Value of Life Contingencies. Philos. Trans. R. Soc. Lond.
344 *115*, 513–583.

345 Grubb, S.C., Bult, C.J., and Bogue, M.A. (2014). Mouse Phenome Database. Nucleic Acids Res. *42*,
346 D825–D834.

347 He, S., and Sharpless, N.E. (2017). Senescence in Health and Disease. Cell *169*, 1000–1011.

348 Helman, A., Klochendler, A., Azazmeh, N., Gabai, Y., Horwitz, E., Anzi, S., Swisa, A., Condiotti, R.,
349 Granit, R.Z., Nevo, Y., et al. (2016). p16(Ink4a)-induced senescence of pancreatic beta cells
350 enhances insulin secretion. Nat. Med. *22*, 412–420.

351 Herbig, U., Ferreira, M., Condel, L., Carey, D., and Sedivy, J.M. (2006). Cellular senescence in
352 aging primates. Science *311*, 1257.

353 Hoeijmakers, J.H.J. (2009). DNA Damage, Aging, and Cancer. N. Engl. J. Med. *361*, 1475–1485.

354 Hwang, H.V., Tran, D.T., Rebuffatti, M.N., Li, C.-S., and Knowlton, A.A. (2018). Investigation of
355 quercetin and hyperoside as senolytics in adult human endothelial cells. PloS One *13*, e0190374.

356 Jeon, O.H., Kim, C., Laberge, R.-M., Demaria, M., Rathod, S., Vasserot, A.P., Chung, J.W., Kim,
357 D.H., Poon, Y., David, N., et al. (2017). Local clearance of senescent cells attenuates the
358 development of post-traumatic osteoarthritis and creates a pro-regenerative environment. Nat.
359 Med. *23*, 775–781.

360 Karlseder, J., Smogorzewska, A., and de Lange, T. (2002). Senescence induced by altered
361 telomere state, not telomere loss. Science *295*, 2446–2449.

362 Kirkland, J.L., and Tchkonia, T. (2015). Clinical strategies and animal models for developing
363 senolytic agents. Exp. Gerontol. *68*, 19–25.

364 Kirkland, J.L., Tchkonia, T., Zhu, Y., Niedernhofer, L.J., and Robbins, P.D. (2017). The clinical
365 potential of senolytic drugs. J. Am. Geriatr. Soc. *65*, 2297–2301.

366 Kirkwood, T.B.L. (2015). Deciphering death: a commentary on Gompertz (1825) 'On the nature
367 of the function expressive of the law of human mortality, and on a new mode of determining
368 the value of life contingencies.' Phil Trans R Soc B *370*, 20140379.

369 Labbadia, J., and Morimoto, R.I. (2015). The biology of proteostasis in aging and disease. Annu.
370 Rev. Biochem. *84*, 435–464.

371 Liu, Y., Sanoff, H.K., Cho, H., Burd, C.E., Torrice, C., Ibrahim, J.G., Thomas, N.E., and Sharpless,
372 N.E. (2009). Expression of p16INK4a in peripheral blood T-cells is a biomarker of human aging.
373 Aging Cell *8*, 439–448.

374 López-Otín, C., Blasco, M.A., Partridge, L., Serrano, M., and Kroemer, G. (2013). The Hallmarks of
375 Aging. Cell *153*, 1194–1217.

376 MacRae, S.L., Croken, M.M., Calder, R.B., Aliper, A., Milholland, B., White, R.R., Zhavoronkov, A.,
377 Gladyshev, V.N., Seluanov, A., Gorbunova, V., et al. (2015). DNA repair in species with extreme
378 lifespan differences. Aging *7*, 1171–1182.

379 Melk, A., Schmidt, B.M.W., Takeuchi, O., Sawitzki, B., Rayner, D.C., and Halloran, P.F. (2004).
380 Expression of p16INK4a and other cell cycle regulator and senescence associated genes in aging
381 human kidney. Kidney Int. *65*, 510–520.

382 Muñoz-Espín, D., and Serrano, M. (2014). Cellular senescence: from physiology to pathology.
383 Nat. Rev. Mol. Cell Biol. *15*, 482–496.

384 Nelson, G., Wordsworth, J., Wang, C., Jurk, D., Lawless, C., Martin-Ruiz, C., and von Zglinicki, T.
385 (2012). A senescent cell bystander effect: senescence-induced senescence. Aging Cell *11*, 345–
386 349.

387 Nelson, G., Kucheryavenko, O., Wordsworth, J., and von Zglinicki, T. (2018). The senescent
388 bystander effect is caused by ROS-activated NF-κB signalling. Mech. Ageing Dev. *170*, 30–36.

389 Ogrodnik, M., Miwa, S., Tchkonia, T., Tiniakos, D., Wilson, C.L., Lahat, A., Day, C.P., Burt, A.,
390 Palmer, A., Anstee, Q.M., et al. (2017). Cellular senescence drives age-dependent hepatic
391 steatosis. Nat. Commun. *8*, 15691.

392 Ogrodnik, M., Salmonowicz, H., and Gladyshev, V.N. (2018). Integrating cellular senescence with
393 the concept of damage accumulation in aging: Relevance for clearance of senescent cells. Aging
394 Cell e12841.

395 Ovadya, Y., and Krizhanovsky, V. (2018). Strategies targeting cellular senescence. J. Clin. Invest.
396 *128*, 1247–1254.

397 Roos, C.M., Zhang, B., Palmer, A.K., Ogrodnik, M.B., Pirtskhalava, T., Thalji, N.M., Hagler, M.,
398 Jurk, D., Smith, L.A., Casaclang-Verzosa, G., et al. (2016). Chronic senolytic treatment alleviates
399 established vasomotor dysfunction in aged or atherosclerotic mice. Aging Cell *15*, 973–977.

400 Sagiv, A., Bar-Shai, A., Levi, N., Hatzav, M., Zada, L., Ovadya, Y., Roitman, L., Manella, G., Regev,
401 O., Majewska, J., et al. (2018). p53 in Bronchial Club Cells Facilitates Chronic Lung Inflammation
402 by Promoting Senescence. Cell Rep. *22*, 3468–3479.

403 Salama, R., Sadaie, M., Hoare, M., and Narita, M. (2014). Cellular senescence and its effector
404 programs. Genes Dev. *28*, 99–114.

405 Schafer, M.J., White, T.A., Iijima, K., Haak, A.J., Ligresti, G., Atkinson, E.J., Oberg, A.L., Birch, J.,
406 Salmonowicz, H., Zhu, Y., et al. (2017). Cellular senescence mediates fibrotic pulmonary disease.
407 Nat. Commun. *8*, 14532.

408 Scheffer, M., Bascompte, J., Brock, W.A., Brovkin, V., Carpenter, S.R., Dakos, V., Held, H., Nes,
409 E.H. van, Rietkerk, M., and Sugihara, G. (2009). Early-warning signals for critical transitions.
410 Nature *461*, 53–59.

411 Scudellari, M. (2017). To stay young, kill zombie cells. Nat. News *550*, 448.

412 Shay, J.W., and Wright, W.E. (2004). Senescence and immortalization: role of telomeres and
413 telomerase. Carcinogenesis *26*, 867–874.

414 Sofue, T., Kushida, Y., Ozaki, T., Moritoki, M., Nishijima, Y., Ohsaki, H., Ueda, N., Kakehi, Y.,
415 Nishiyama, A., and Minamino, T. (2018). Tubular Cell Senescence in the Donated Kidney Predicts
416 Allograft Function, but Not Donor Remnant Kidney Function, in Living Donor Kidney
417 Transplantation. Am. J. Nephrol. *47*, 8–17.

418 Solana, R., Tarazona, R., Gayoso, I., Lesur, O., Dupuis, G., and Fulop, T. (2012). Innate
419 immunosenescence: effect of aging on cells and receptors of the innate immune system in
420 humans. In Seminars in Immunology, (Elsevier), pp. 331–341.

421 Stroustrup, N., Anthony, W.E., Nash, Z.M., Gowda, V., Gomez, A., López-Moyado, I.F., Apfeld, J.,
422 and Fontana, W. (2016). The temporal scaling of Caenorhabditis elegans ageing. Nature *530*,
423 103–107.

424 Van Deursen, J.M. (2014). The role of senescent cells in ageing. Nature *509*, 439.

425 Vaupel, J.W. (1998). Biodemographic Trajectories of Longevity. Science *280*, 855–860.

426 Von Zglinicki, T., Saretzki, G., Ladhoff, J., di Fagagna, F. d'Adda, and Jackson, S.P. (2005). Human
427 cell senescence as a DNA damage response. Mech. Ageing Dev. *126*, 111–117.

428 Weitz, J.S., and Fraser, H.B. (2001). Explaining mortality rate plateaus. Proc. Natl. Acad. Sci. *98*,
429 15383–15386.

430 Xu, M., Palmer, A.K., Ding, H., Weivoda, M.M., Pirtskhalava, T., White, T.A., Sepe, A., Johnson,
431 K.O., Stout, M.B., Giorgadze, N., et al. (2015). Targeting senescent cells enhances adipogenesis
432 and metabolic function in old age. ELife *4*, e12997.

433 Xu, M., Pirtskhalava, T., Farr, J.N., Weigand, B.M., Palmer, A.K., Weivoda, M.M., Inman, C.L.,
434 Ogrodnik, M.B., Hachfeld, C.M., Fraser, D.G., et al. (2018). Senolytics improve physical function
435 and increase lifespan in old age. Nat. Med.

436 Yosef, R., Pilpel, N., Tokarsky-Amiel, R., Biran, A., Ovadya, Y., Cohen, S., Vadai, E., Dassa, L.,
437 Shahar, E., Condiotti, R., et al. (2016). Directed elimination of senescent cells by inhibition of
438 BCL-W and BCL-XL. Nat. Commun. *7*, 11190.

439 Young, A.R., and Narita, M. (2009). SASP reflects senescence. EMBO Rep. *10*, 228–230.

440 Zhou, S., Greenberger, J.S., Epperly, M.W., Goff, J.P., Adler, C., Leboff, M.S., and Glowacki, J.
441 (2008). Age-related intrinsic changes in human bone-marrow-derived mesenchymal stem cells
442 and their differentiation to osteoblasts. Aging Cell *7*, 335–343.

443 Zhu, Y., Tchkonia, T., Pirtskhalava, T., Gower, A.C., Ding, H., Giorgadze, N., Palmer, A.K., Ikeno, Y.,
444 Hubbard, G.B., and Lenburg, M. (2015). The Achilles' heel of senescent cells: from transcriptome
445 to senolytic drugs. Aging Cell *14*, 644–658.

446 Zhu, Y., Tchkonia, T., Fuhrmann-Stroissnigg, H., Dai, H.M., Ling, Y.Y., Stout, M.B., Pirtskhalava, T.,
447 Giorgadze, N., Johnson, K.O., and Giles, C.B. (2016). Identification of a novel senolytic agent,
448 navitoclax, targeting the Bcl-2 family of anti-apoptotic factors. Aging Cell *15*, 428–435.

449 Zhu, Y., Doornebal, E.J., Pirtskhalava, T., Giorgadze, N., Wentworth, M., Fuhrmann-Stroissnigg,
450 H., Niedernhofer, L.J., Robbins, P.D., Tchkonia, T., and Kirkland, J.L. (2017). New agents that
451 target senescent cells: the flavone, fisetin, and the BCL-XL inhibitors, A1331852 and A1155463.
452 Aging *9*, 955.

453

454

455

456

457